Frequency Response of Acoustic-Assisted Ni–Mn–Ga Ferromagnetic-Shape-Memory-Alloy Actuator

Ratchatee Techapiesancharoenkij[1,2], Jari Kostamo[3], Samuel M. Allen[1] and Robert C. O'Handley[1,4]

[1] Department of Materials Science and Engineering, Massachusetts Institute of Technology, Cambridge, Massachusetts 02139, USA

[2] Department of Materials Engineering, Faculty of Engineering, Kasetsart University, Bangkok 10900, Thailand

[3] Machine Design, Helsinki University of Technology, FI-02015 TKK, Finland

[4] Ferro Solutions, Inc., Woburn, Massachusetts 1801, USA

ABSTRACT

A prototype of Ni–Mn–Ga based ferromagnetic-shape-memory-alloy (FSMA) actuator was designed and built; an acoustic-assist technique was applied to the actuator to enhance its performance. A piezoelectric stack actuator was attached to the Ni–Mn–Ga sample to generate acoustic energy to enhance twin-boundary mobility and, hence, reduce the magnetic threshold field required for activating twin-boundary motion. The dynamic response of the acoustic-assist FSMA actuator was measured up to 1-kHz actuation. The acoustic assistance improves the actuator performance, by increasing the reversible magnetic-field-induced strain (MFIS) by up to 100% (increase from 0.017 to 0.03 at 10 Hz), for drive frequencies below 150 Hz. For frequencies above 150 Hz, the acoustic-assist effect becomes negligible and the resonant characteristic of the actuator takes over the actuator response. Even though the acoustic assist does not improve the actuation at high frequencies, the MFIS output of 5% can be obtained at the resonant

frequency of 450 Hz. The FSMA actuator is shown to be ideal for applications that require large strain at a specific high frequency.

Introduction

Ferromagnetic shape memory alloys (FSMAs) have emerged as a promising class of active materials due to their large magnetic-field-induced strain (MFIS) [1-4]. They can potentially be actuated at frequencies up to 2 kHz [5]. An off-stoichiometric martensitic Ni_2MnGa single crystal, the most-studied alloy in the FSMA class, exhibits large strain up to ε_o, = 1 –c/a where ε_o is the strain across a twin boundary and c/a is a ratio of the short crystallographic c-axis to the long a-axis; the theoretical maximum MFIS are 0.06 and 0.1 for tetragonal and orthorhombic Ni–Mn–Ga single crystals, respectively [4]. MFIS from a Ni-Mn-Ga FSMA is comparable to that of conventional shape memory alloy (SMA) and more than ten times larger than that of piezoelectric or magnetostrictive materials. Its potential actuating frequency is much higher than that of SMA, which is limited by heat-transfer-dependent transformation processes. MFIS occurs via twin-boundary motion. It requires that the magnetic anisotropy energy of the FSMA crystal be larger than the energy required for activating twin boundary motion. The direction of the magnetic easy axis in the tetragonal phase is the crystallographic short c-axis. This axis changes its orientation by almost 90^o from one variant (V1) to the other variant (V2) across the twin boundary. Application of a magnetic field perpendicular to the easy axis of variant V1 favors the motion of the twin boundaries through the sample in a direction that would grow variant V2, which has the easy axis parallel to the field direction [6,7].

Ni-Mn-Ga FSMAs still have some limitations that may prevent them from being applied in commercial actuator devices. It has been shown that a *threshold* field of 1 – 3 kOe (depending on sample shape and condition) is required to activate twin-boundary

motion and a larger *saturating* field of approximately 6.5 kOe is needed to achieve full MFIS [3,8,9]. Such magnetic fields require an electromagnet that is large compared to the active material volume and can account for more than 95% of the total mass of the actuator device.

The other drawback of FSMAs is that the twin boundary motion, and hence MFIS, is an irreversible process. As a result, to obtain a reversible MFIS (especially in dynamic applications), an external stress or magnetic field must be applied to compressively reset an FSMA sample after it is magnetically extended. The magnetic stress must then be used to move twin boundaries and to extend the FSMA against the external bias stress and load. The maximum magnetic energy that can be coupled into the tetragonal NiMnGa material is limited by the anisotropy energy, $K_u \sim 1.5 \times 10^5$ J/m^3 (at room temperature). For twin boundary motion to occur, $K_u/\varepsilon_o \sim 2.5$ MPa must exceed the sum of the bias, load and defect stresses [5,8,10]. This limitation results in a reduction in an output strain relative to that of the unstressed state. Henry et al. studied the dynamic actuation of a Ni–Mn–Ga single crystal and observed only up to 3% cyclic strains with an AC magnetic field of 6.5 kOe amplitude [11]. The magnetic anisotropy energy is temperature-dependent; it decreases almost linearly with increasing temperature, reaching zero at $T = T_C$, of the FSMA[12-14]. Consequently, the magnetic stress output may increase if the operating temperature is much lower than the Curie temperature. Karaca et al. reported a large magnetic stress of 5.7 MPa with the maximum MFIS of 5.8% under an application of the magnetic-field amplitude of 16 kG for martensitic NiMnGa alloys operated at -95 ^{o}C; the magnetocrystalline anisotropy energy at -95 ^{o}C was calculated to be 3.3×10^5 J/m^3 [14].

A higher magnetic stress of the FSMA may also be obtained by increasing the amount of energy required for the magnetization rotation process in addition to the magnetocrystalline anisotropy. Ganor et al. demonstrates theoretically and experimentally that the energy barrier for magnetization rotation may be increased by reducing the FSMA sample's size (I don't understand this size dependence without rading the Ganor paper but, you can probably say what you do say). With the increase in the energy barrier to magnetization rotation, the variant reorientation via twin boundary motion is more favorable than the magnetization rotation; as a result, higher magnetostress can be coupled to the magnetic actuation of an FSMA material resulting in higher blocking stress. A single crystal Ni_2MnGa sample with square cross section of 200 × 200 micron and a length of 4 mm was actuated at -28 ^{o}C (30 ^{o}C below its martensitic-finish temperature) with increasing mechanical load; a blocking stress of up to 10 MPa can be achieved with this sample [15].

We report a means to reduce the required threshold field and increase the strain output at room temperature without altering the FSMA dimensions or reducing its temperature. It has been reported that application of an acoustic wave (from a piezoelectric stack transducer) with an appropriate polarization, to the Ni-Mn-Ga single crystal during the MFIS actuation at low frequencies (≤ 1 Hz) can result in a reduction of the threshold field by up to 0.5 kOe and a significant increase in the strain output depending on the magnetic field [16-18]. It is also reported that the cyclic reversible strain of the Ni-Mn-Ga single crystal increases from 0.03 to 0.045 with an acoustic-assist technique. The larger strain appears over a broader range of stress output [17]. As a

result, the acoustic-assist technique is shown to increase the efficiency of an FSMA device in delivering mechanical energy $\sigma_{bias}\varepsilon_{out}$.

To date, the reports on the acoustic-assist effect on Ni-Mn-Ga single crystal actuation all treat quasi-static or low-frequency (< 10 Hz) conditions. In this work, we study the acoustic-assist effect on MFIS at higher frequency from 10 Hz to 1 kHz. A prototype FSMA actuator was designed and built having a piezoelectric stack actuator that provides acoustic energy to assist twin boundary motion. To further enhance its actuating performance, the commonly used coil spring was replaced by a disc spring to minimize unwanted buckling of the load path. Coil springs are prone to bending modes at low frequency (as low as 100 Hz) as observed in previous studies [11,19,20]. The electromagnet is also built to minimize the gap width so that the magnet pole pieces are as close to the FSMA as possible. As a result, the magnetic field strength through the sample is larger for a given current.

In what follows, we briefly describe the FSMA actuator that was designed and built for this study. The electromagnetic performance over frequency range from 10 to 1000 Hz is also tested and shown. The results of the frequency response of the acoustic-assisted FSMA actuator with an application of an AC magnetic-field amplitude of 3.5 kOe over the same frequency range is also described followed by a discussion of their implications. In the final section, the conclusions of this report are summarized.

Experimental Procedure

The acoustic-assisted FSMA actuator used in this study is shown in Figure 6. A tetragonal $Ni_{50.3at\%}Mn_{28.2at\%}Ga_{21.5at\%}$ single crystal, grown by the Bridgman method

Ref[21], was cut with faces parallel to the austenitic {100} planes and dimensions of 16 mm x 4 mm x 2 mm. The Ni–Mn–Ga crystal was placed between the electromagnet poles; the pole faces were larger than the 16 x 4 mm faces of the crystal and the magnet gap was marginally larger than 2 mm width of the crystal. Two 33-mode piezoelectric stack actuators were used, one attached to each end of the crystal. Two flexural disc springs, with a spring constant of 26.5 kN/m, were connected at the outer end of each piezoelectric stack to compressively bias the crystal. Under the application of the AC magnetic field, the Ni–Mn–Ga crystal extends and contracts with a nodal (stationary) plane at the center of the sample. During actuation with acoustic assistance, the piezoelectric stack was driven at 40 $V_{p\text{-}p}$ and 7 kHz; the choice of these voltage and frequency values is based on a previous report showing that the optimal acoustic-assist effect can be obtained at these values [18]. Two capacitive proximity probes were used, one outside each disc spring, to measure the displacements on left and right hand sides of the actuator load line. The total elongation of the Ni–Mn–Ga crystal is the sum of the displacements on the two sides.

The flexural disc springs were used to avoid the buckling problem often encountered with the usage of a coil spring [19,20]. The symmetrically-actuating design with nodal plane at the center of the Ni–Mn–Ga crystal allows for the use of two piezoelectric stacks to double the acoustic-assist effect on the twin-boundary motion. The elliptical clamps surrounding the piezoelectric stacks provide bias compressive stresses to improve the piezoelectrics' performance and prevent debonding or fracture between the piezoceramic layers without applying additional bias stress to the FSMA.

The electromagnet consists of a laminated, soft magnetic core and insulated copper-wire winding. The electromagnet performance was tested over the frequency range from 10 Hz to 1 kHz. It was driven with a sinusoidal current waveform with specific *input*-current amplitude from the power amplifier in current controlled mode at varying frequencies. The actual *output* current flowing through the winding coils was then measured and plotted against frequency (Figure 7). The electromagnet can be driven up to a current of 5-A without a significant drop in the current output over the studied frequency range. Above 5-A, the output current decreases significantly once the drive frequencies are above 500 Hz. For example, the current output from 9-A current drive drops to 4 A at 1 kHz. The power supply was capable of supplying the programmed current at low frequencies. However, there were a sufficient number of turns in the coils that at higher frequencies the higher inductance of the coils reduced the maximum achievable output current at higher frequencies. The maximum supply voltage was 100 V, which is not sufficient to drive the current above 5 A at frequencies above 500 Hz. Therefore, the actual output current amplitude is lower than the programmed input current amplitude above 5 A at high frequencies. The current-drive amplitude of 5 A is therefore used in this study to ensure a uniform magnetic-field strength, throughout the studied frequency range; a 5-A current drive provides a magnetic-field amplitude of 3.5 kOe (almost 40% below a typical saturating field). It should be noted that the magnetic-field amplitude in this work is lower than that in Ref. [11] by 3 kOe.

To avoid temperature rise due to eddy current heating and/or twin-boundary motion dissipative heat, for given frequency, the actuator was driven for 5 seconds for MFIS measurement and then rested for 15 seconds. The temperature of the FSMA

sample was monitored to ensure that the temperature was within ± 1 ^{o}C of room temperature during actuation.

Results and Discussion

Figure 8 shows MFIS-vs.-magnetic field at 10 Hz actuation with and without acoustic assistance. The acoustic assistance significantly improves the MFIS response of the FSMA actuator by decreasing the required threshold field by 0.7 kOe and increasing the cyclic MFIS from 1.7% to 3.1% with the magnetic-field amplitude of 3.5 kOe. In Ref. [11], the maximum cyclic MFIS achieved at 1 Hz drive is 2.7% with a maximum field as high as 6.5 kOe.

The cyclic MFIS under 3.5 kOe peak magnetic field was measured for increasing drive-field frequencies up to 1 kHz, as shown in Figure 9. The frequency response shows that the FSMA actuator studied here has a resonant frequency at 450 Hz. The maximum MFIS increases from 2% at 10 Hz to 5% at 450 Hz for a constant 3.5 kOe amplitude drive.

It is clear from Fig. 4 that the acoustic assistance is useful only at low frequency drive (lower than 100 Hz). A 3.5% MFIS may be achieved at a magnetic field drive as low as 3.5 kOe. The reduction in threshold field can reduce significantly the size of the electromagnet required for actuation. However, at high drive frequency, the acoustic-assist effect is negligible. The cyclic MFIS of the FSMA actuator with and without acoustic assistance are almost identical across the frequency range from 200 Hz to 1 kHz. The FSMA actuator appears to be governed in this frequency range by the resonant

characteristic of the system. As shown in

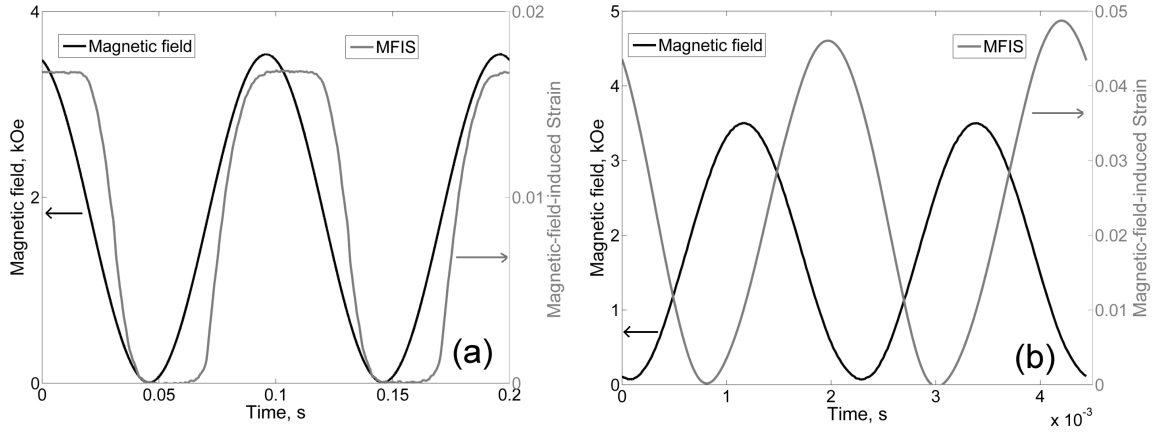

Figure 10(a), at 10 Hz (quasi-static condition), the MFIS response over time is non-harmonic and does not follow the sinusoidal response of the magnetic field drive. The MFIS remains zero when the field is lower than the threshold field and then rises to maximum for H ≈ 3.3 – 3.4 kOe. Further increase in magnetic field produces no significant increase in MFIS. As the field decreases, the MFIS remains at its maximum level until the field decreases below the reset threshold field. The MFIS response of the FSMA actuator is governed by the non-linear response of the FSMA sample. At 450 Hz (

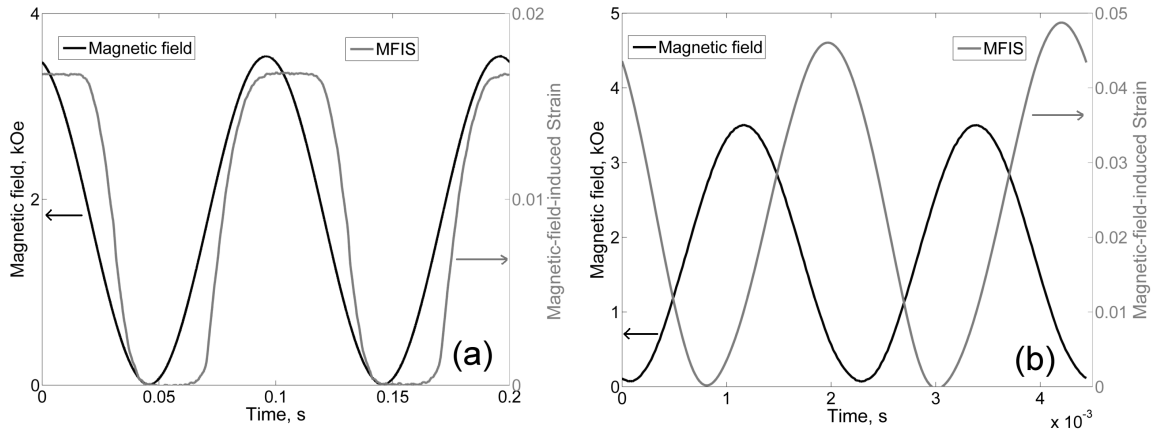

Figure 10(b)), both MFIS and magnetic field respond sinusoidally over time. A smooth sinusoidal response of MFIS is obtained and not hindered by the threshold-field characteristic typically observed at quasi-static condition..

The decrease of the acoustic-assist effect at higher frequencies may be due to two factors. The first is clearly the dynamic behavior of the actuator system. In a dynamic system, the inertia and damping forces become more significant than the acoustic stress

waves. As the system's frequency approaches resonance, the driven magnetic actuation constructively increases the strain output along with the system's vibration. As the system frequency surpasses the resonant frequency, the driven force from the magnetic drive becomes counterproductive to the system's vibration and the total strain decreases. In both cases, the dynamic forces of the systems seem to be little affected by an addition of the acoustic energy.

The second factor that could decrease the acoustic effect for frequencies above about 200 Hz is the lower ratio of acoustic frequency to the magnetic actuation frequency. The piezoelectric drive frequency is constant at 7 kHz while the FSMA actuation frequency increases from 10 to 1000 kHz. As a result, the number of acoustic cycles per magnetic actuation cycle decreases as the magnetic drive frequency increases. Consequently, the piezoelectric stack generates fewer stress waves to help enhance twin-boundary motions per magnetic drive cycle. Unfortunately, increasing the piezoelectric drive frequency is not an option because it is outside the operating frequency of the piezo stack used in this study. It has been shown that the displacement of the piezo stack decreases significantly as the drive frequency is above 5 kHz; as a result, the acoustic stress wave amplitude also decreases [18].

The load amplitude from this actuator may be estimated to be equal to the product of the spring constant (= 26.5 kN/m) and the displacement amplitude (= MFIS x the sample's length). The load amplitude of the actuator without acoustic assistance at low frequency (10 Hz) is calculated to be 7.95 N or 0.99 MPa. The resulting load corresponds well with the previous report [17] that, under quasi-static actuation, the stress output from FSMA actuators is typically limited in the range between 0.8 – 1.5 MPa,

because the magnetic energy that is coupled into a material is limited by the anisotropy energy, K_u.

The load amplitude at the resonant frequency of 450 Hz is approximately 21.2 N or 2.6 MPa. The higher load amplitude at resonant frequency than those at quasi-static conditions is due to the dynamic behavior of the system at resonance. However, at frequencies above the resonant frequency, the displacement drops significantly and, as a result, the load amplitude decreases dramatically. For example, at 1 kHz, the estimated load amplitude from this actuator decreases to 2.65 N or 0.33 MPa.

The work density output of the actuator is equal to $\sigma_m\varepsilon_m/2$ where σ_m and ε_m the amplitudes of the stress and strain outputs, respectively. The work-density output as a function of the magnetic drive frequency is plotted in Figure 6. At 10 Hz, the acoustic assistance increases the work output by 7 kJ/m^3. The acoustic assistance has no effect on the work output for frequencies above 150 Hz. At resonant frequency, the work output is maximum and approximately equal to 65 kJ/m^3.

The efficiency of the energy transmission from the piezoelectric stack to the FSMA crystal's actuation is considered for a 10-Hz magnetic drive. The electrical energy stored in the piezo stack is equal to $CV^2/2$. The capacitance (C) of the piezo stack is 1600 nF and the applied peak-to-peak voltage (V) is 40 V; thus, the electrical energy stored in the piezo stack is approximately 1.28 mJ. At 10 Hz magnetic actuation, the mechanical-work output of the FSMA actuator (= work density × sample's volume) is increased, due to the acoustic assistance, by 0.9 mJ. The mechanical-work gain of the FSMA actuation with the acoustic assistance is clearly lower than the actual electrical

energy stored in the piezoelectric stack. We have no way of knowing how much of the stored energy is actually transmitted to the FSMA.

In our current setup, the piezoelectric stack is directly attached to the FSMA sample. The acoustic impedances of the stack and the FSMA sample are significantly different (e.g. different cross-sectional areas, modulus and density). As a result, the acoustic energy transmission is not optimal due to acoustic mismatch between the two mediums. The energy-transmission efficiency may be improved by introducing a better acoustic-match tuner in between the FSMA sample and the piezo stack.

The acoustic assistance may not improve the total efficiency of energy conversion from the electrical (acoustic drive) and magnetic (magnetic field) energy to the mechanical energy (FSMA work output), because the acoustic energy input is not completely converted into a mechanical energy output. Yet, for low frequency actuations (below 150 Hz), the acoustic assistance can be an immediate help to make an FSMA actuator more compact by reducing the required magnetic field and, hence, the size of the electromagnet coils. For high frequency actuations, the acoustic assistance does not reduce the required threshold magnetic field or improve the FSMA work output; as a result, the acoustic-assist technique is not useful for high-frequency FSMA application.

Conclusion

A FSMA actuator was built and tested. It provides magnetic-field-induced actuation with an acoustic assist provided by a piezoelectric stack actuator. The actuator studied here is further improved by use of a disc spring and minimum gap between the magnetic poles. The actuator generates strain of 5% with drive magnetic field amplitude

of 3 kOe at 450 Hz. Previously-reported FSMA actuators typically achieve up to 3% strain with required magnetic field amplitude of 6 kOe.

The acoustic assistance helps increase the MFIS and work output significantly for magnetic drive frequencies lower than 150 Hz. As the frequency approaches the resonant frequency, the acoustic-assist effect disappears.

Even though the acoustic-assistance has a negligible effect at high frequency, the prototype FSMA actuator is shown to provide MFIS output as high as 5% at 450 Hz. It appears that this is the highest MFIS reported to date at this high frequency of 450 Hz. Previously reported maximum dynamic MFIS is only 3% at maximum frequency of 200 Hz. Moreover, the magnetic field amplitude used in this study is also smaller than that in Ref [11] by 20%. The current design including the usage of disc spring and smaller gap of electromagnetic pole is proved to enhance FSMA performance effectively.

The study shows that one can obtain large MFIS at higher frequencies using resonant characteristics of the actuator system. The FSMA actuator is shown to be ideal for applications that require large strain at a specific high frequency.

Acknowledgement

This work was supported by a Multi-University Research Initiative sponsored by the Office of Naval Research (ONR), Grant No. N0014-01-0758, and by a subcontract from Ferro Solutions, Inc. on ONR STTR Phase I and Phase II contracts.

References

[1] K. Ullakko, J. Huang, C. Kantner, R. OHandley, and V. Kokorin, "Large magnetic-field-induced strains in Ni2MnGa single crystals," *Appl Phys Lett*, vol. 69, Sep. 1996, pp. 1966-1968.
[2] R. James, R. Tickle, and M. Wuttig, "Large field-induced strains in ferromagnetic shape memory materials," *Mat. Sci. Eng. A*, vol. 273-275, 1999, pp. 320-325.
[3] S. Murray, M. Marioni, S. Allen, R. O'Handley, and T. Lograsso, "6% magnetic-field-induced strain by twin-boundary motion in ferromagnetic Ni-Mn-Ga," *Appl Phys Lett*, vol. 77, Aug. 2000, pp. 886-888.
[4] A. Sozinov, A. Likhachev, N. Lanska, and K. Ullakko, "Giant magnetic-field-induced strain in NiMnGa seven-layered martensitic phase," *Appl Phys Lett*, vol. 80, Mar. 2002, pp. 1746-1748.
[5] M. Marioni, R. O'Handley, and S. Allen, "Pulsed magnetic field-induced actuation of Ni-Mn-Ga single crystals," *Appl Phys Lett*, vol. 83, Nov. 2003, pp. 3966-3968.
[6] R. James and M. Wuttig, "Magnetostriction of martensite," *Philos Mag A*, vol. 77, May. 1998, pp. 1273-1299.
[7] R. O'Handley, "Model for strain and magnetization in magnetic shape-memory alloys," *J Appl Phys*, vol. 83, Mar. 1998, pp. 3263-3270.
[8] A. Likhachev and K. Ullakko, "Magnetic-field-controlled twin boundaries motion and giant magneto-mechanical effects in Ni-Mn-Ga shape memory alloy," *Phys Lett A*, vol. 275, Oct. 2000, pp. 142-151.
[9] O. Heczko, A. Sozinov, and K. Ullakko, "Giant field-induced reversible strain in magnetic shape memory NiMnGa alloy," *Magnetics, IEEE Transactions on*, vol. 36, 2000, pp. 3266-3268.
[10] O. Heczko and L. Straka, "Giant magneto-elastic strain - magnetic shape memory effect," *Czechoslovak Journal of Physics*, vol. 54, 2004, pp. D611-D614.
[11] C.P. Henry, D. Bono, J. Feuchtwanger, S.M. Allen, and R.C. O'Handley, "ac field-induced actuation of single crystal Ni--Mn--Ga," *J. Appl. Phys.*, AIP, 2002, pp. 7810-7811.
[12] L. Straka and O. Heczko, "Magnetic anisotropy in Ni-Mn-Ga martensites," *J Appl Phys*, vol. 93, May. 2003, pp. 8636-8638.
[13] L. Straka, O. Heczko, and S. Hannula, "Temperature dependence of reversible field-induced strain in Ni-Mn-Ga single crystal," *Scripta Mater* , vol. 54, Apr. 2006, pp. 1497-1500.
[14] H. Karaca, I. Karaman, B. Basaran, Y. Chumlyakov, and H. Maier, "Magnetic field and stress induced martensite reorientation in NiMnGa ferromagnetic shape memory alloy single crystals," *Acta Materialia*, vol. 54, Jan. 2006, pp. 233-245.
[15] Y. Ganor, D. Shilo, T.W. Shield, and R.D. James, "Breaching the work output limitation of ferromagnetic shape memory alloys," *Applied Physics Letters*, vol. 93, 2008, pp. 122509-3.
[16] B. Peterson, J. Feuchtwanger, J. Chambers, D. Bono, S. Hall, S. Allen, and R. O'Handley, "Acoustic assisted, field-induced strain in ferromagnetic shape memory alloys," *J Appl Phys*, vol. 95, Jun. 2004, pp. 6963-6964.
[17] R. Techapiesancharoenkij, J. Kostamo, J. Simon, D. Bono, S.M. Allen, and R.C. O'Handley, "Acoustic-assisted magnetic-field-induced strain and stress output of Ni--Mn--Ga single crystal," *Applied Physics Letters*, vol. 92, Jan. 2008, pp. 032506-3.

[18] R. Techapiesancharoenkij, J. Simon, D. Bono, S.M. Allen, and R.C. O'Handley, "Acoustic-assist effect on magnetic threshold field and twinning-yield stress of Ni--Mn--Ga single crystals," *Journal of Applied Physics*, vol. 104, 2008, pp. 033907-6.
[19] C. Henry, "Dynamic actuation properties of Ni-Mn-Ga ferromagnetic shape memory alloys," Massachusetts Institute of TechnologyEditor, 2002.
[20] B. Peterson, "Acoustic Assisted Actuation of Ni-Mn-Ga Ferromagnetic Shape Memory Alloys," Massachusetts Institute of Technology, 2006.
[21] D. Schlagel, Y. Wu, W. Zhang, and T. Lograsso, "Chemical segregation during bulk single crystal preparation of Ni-Mn-Ga ferromagnetic shape memory alloys," *J Alloy Compd*, vol. 312, Nov. 2000, pp. 77-85.

List of Figure Captions

Figure 1: Photograph of the acoustic-assisted FSMA actuator (top) and a schematic illustration of the corresponding actuator (bottom).

Figure 2: The electromagnet performance as a function of frequency at different programmed input-current amplitudes.

Figure 3: Magnetic-field-induced strain (MFIS) as a function of the magnetic field at 10 Hz actuation with and without acoustic assistance.

Figure 4: The cyclic MFIS over frequency range from 10 Hz to 1 kHz.

Figure 5: Magnetic field and MFIS-vs.-time for (a) 10 Hz and (b) 450 Hz FSMA actuation.

Figure 6: Work-density output of the FSMA actuator as a function of the drive frequency of the magnetic field.

Figures

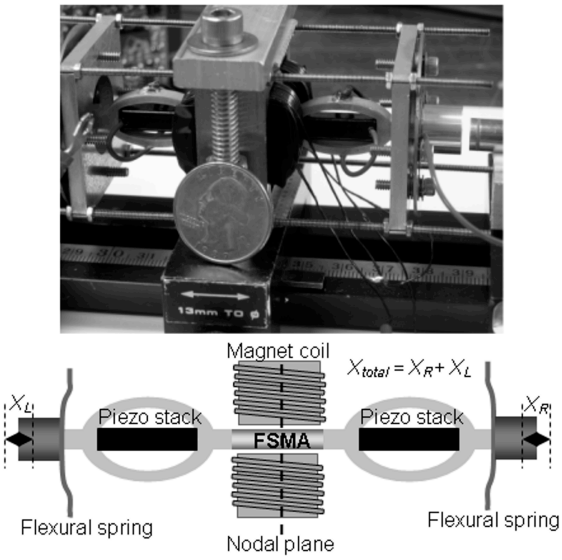

Figure 6: Photograph of the acoustic-assisted FSMA actuator (top) and a schematic illustration of the corresponding actuator (bottom).

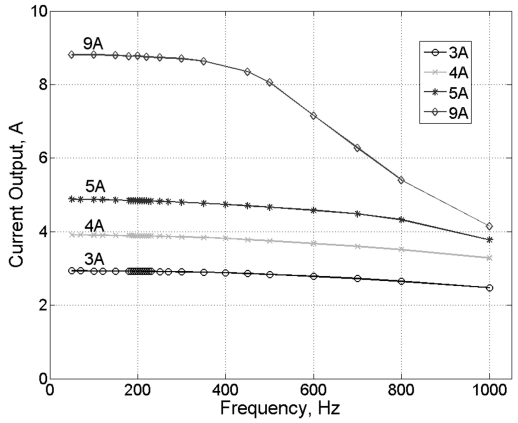

Figure 7: The electromagnet performance as a function of frequency at different programmed input-current amplitudes.

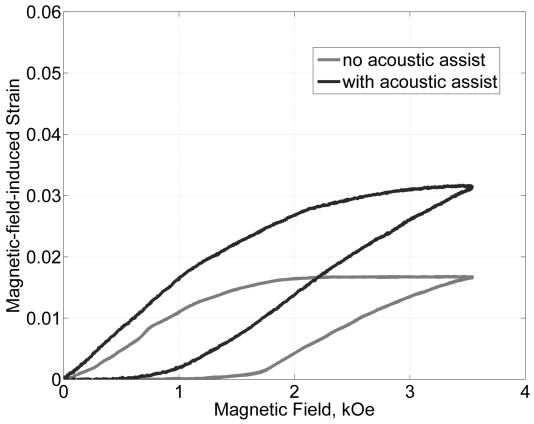

Figure 8: Magnetic-field-induced strain (MFIS) as a function of the magnetic field at 10 Hz actuation with and without acoustic assistance.

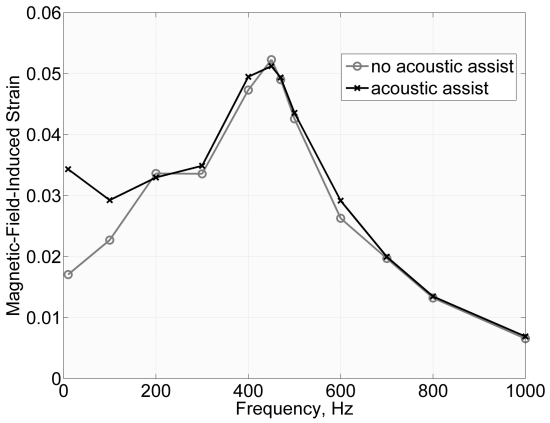

Figure 9: The cyclic MFIS over frequency range from 10 Hz to 1 kHz.

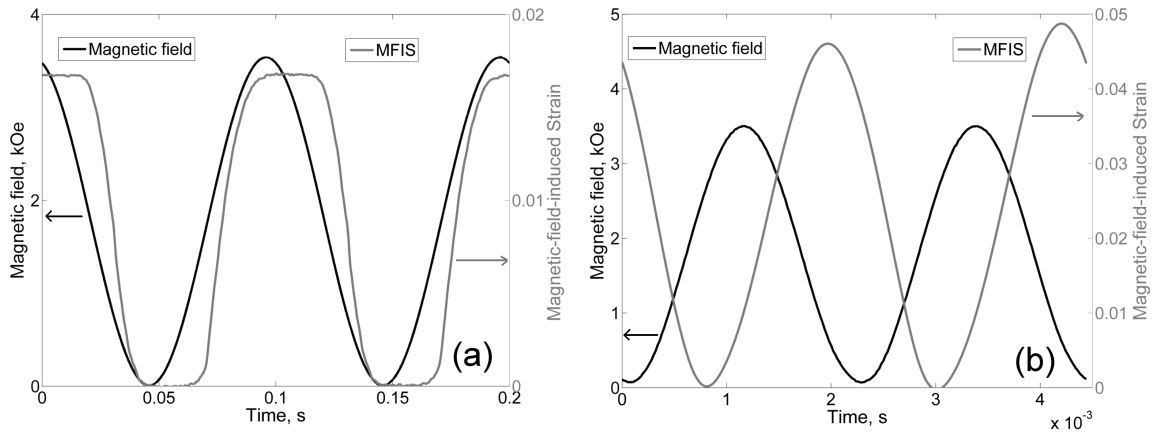

Figure 10: Magnetic field and MFIS-vs.-time for (a) 10 Hz and (b) 450 Hz FSMA actuation.

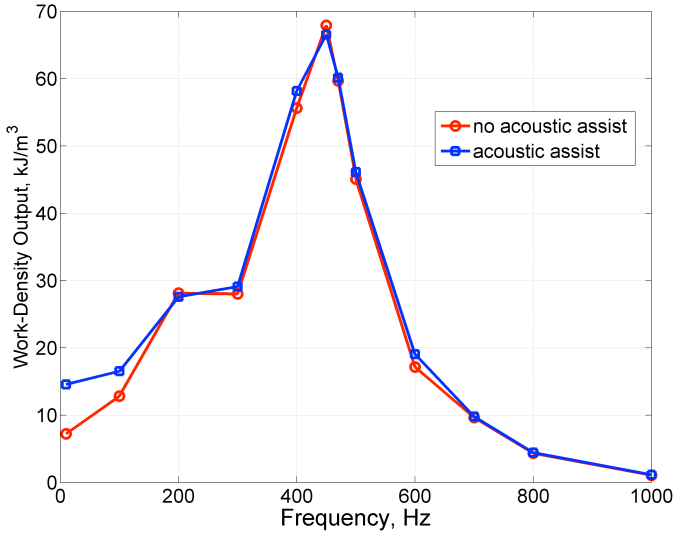

Figure 6: Work-density output of the FSMA actuator as a function of the drive frequency of the magnetic field.